Probabilistic Aircraft Conflict Detection and Resolution Considering Wind Uncertainty

Eulalia Hernández-Romero*, Alfonso Valenzuela† and Damián Rivas‡
Department of Aerospace Engineering
Universidad de Sevilla, 41092 Seville, Spain
Email:*ehernandez9@us.es, †avalenzuela@us.es, ‡drivas@us.es

***Abstract*—A probabilistic aircraft conflict detection and resolution method considering wind uncertainty is proposed in this paper. The wind components are modeled as random variables, described by a joint probability density function. The case of two en-route aircraft flying with constant airspeed in the same airspace and flight level with approaching multi-segment trajectories and affected by the same wind is considered. The conflict is characterized by the minimum distance between the aircraft and the probability of conflict. The probabilistic conflict detection is performed using the Probabilistic Transformation Method. The conflict resolution problem is formulated as a parametric optimization problem subject to constraints, being the optimality criterium the minimization of the spatial deviation from the nominal trajectory. Numerical results are presented for statistically-independent and uniformly distributed constant winds obtained from Ensemble Weather Forecasts.**

I. Introduction

Improving capacity, efficiency, and safety levels of the Air Traffic Management (ATM) system are main goals of both the Single European Sky ATM Research (SESAR) and the Next Generation Transportation System (NextGen). The ever increasing levels of air traffic challenge these goals, making the development and integration of innovative automated decision support tools a necessity.

An approach that can improve prediction and optimization mechanisms is to model, analyze, and manage the uncertainty present in ATM. Among the many sources of uncertainty, the effects of weather uncertainty on the ATM system are of utmost importance, see Rivas and Vazquez [1]. The limited knowledge about future meteorology conditions, such as wind velocity and direction, fog, snowfall or storms, is responsible for much of the delays and flight cancellations, which negatively affects ATM efficiency and translates to extra costs for airlines and air navigation service providers.

Attending to weather conditions, two types of uncertainty can be identified. Firstly, hazardous weather which may lead to no-fly zones affecting the ATM at a network level; and, secondly, some atmospheric properties, particularly the wind, which may affect aircraft individual trajectories. The inclusion and analysis of weather uncertainty into ATM-related problems has been addressed by many authors. For example, Zheng and Zhao [2] developed a statistical model of wind uncertainties and applied it to stochastic trajectory prediction in the case of straight, level flight trajectories at constant airspeed with different guidance laws, which affect the distributions of dispersions of the trajectory attributes. Nilim et al. [3] proposed a dynamic routing strategy for an aircraft that minimizes the expected delay when the aircraft's nominal path may be obstructed by bad weather, obtaining significant improvements when compared with more conservative strategies.

In this paper, a methodology to include the effects of wind uncertainty on the problem of aircraft conflict detection and resolution (CD&R), focused on the cruise phase of the flight, is developed. The CD&R problem under uncertainty has been addressed in the past by several authors. A widely used approach is to consider the aircraft expected position as a random variable and assume it follows a probabilistic distribution: Paielli and Erzberger [4] estimated the probability of conflict for pairs of aircraft whose trajectories were uncertainly predicted, considering the trajectory prediction errors as Gaussian variables; Krozel and Peters [5] presented a non-deterministic conflict detection model for two en-route aircraft, considering their positions, velocities and headings as Gaussian distributions; and Prandini et al. [6] also obtained expressions for the probability of conflict, applying two different models for the tracking errors. Another approach is to propagate the weather uncertainty into the trajectory prediction: Hu et al. [7] and Chaloulos and Lygeros [8] used this approach to study how wind correlation affects conflict probability; Matsuno et al. [9][10] proposed probabilistic aircraft conflict detection and resolution algorithms in the presence of spatially correlated uncertain winds and applied them to the two-dimensional aircraft-aircraft and aircraft-weather conflict resolution problem; and Rodionova et al. [11] developed and evaluated different conflict strategic resolution algorithms for wind-optimal trajectories considering wind uncertainties in the North Atlantic oceanic airspace. This second approach is followed in this paper.

In order to characterize and quantify the uncertainty in a weather forecast, it is convenient to use a probabilistic approach. This paper considers wind uncertainty provided by Ensemble Prediction Systems (EPS), a weather forecasting technique that characterizes and quantifies the uncertainty inherent to the prediction. The EPS has succesfully been applied to Air Traffic Management problems in the past. González-Arribas et al. [12] generated wind-optimal cruise trajectories using pseudospectral methods and studied the sensitivity of the optimal flight paths to the numerical weather prediction uncertainty. Steiner et al. [13] presented an approach, focused on convective storms, of how high-resolution ensemble weather forecasts may get integrated with automated ATM decision support tools. Rivas et al. [14] analyzed the effects of wind uncertainty on aircraft fuel consumption in the case of multi-segment cruise flight subject to average constant winds.

In this paper, the problem of two aircraft flying with approaching trajectories composed of several cruise segments at constant airspeed, constant altitude and affected by the same uncertain winds is tackled. The conflict detection is based on the Probabilistic Transformation Method (PTM), see for example Hogg and Craig [15]. A first step on the assessment of the impact of wind uncertainty on the problem of conflict detection using this method was presented in Hernández et al. [16]. The conflict resolution problem is formulated as a parametric optimization problem subject to constraints, being the optimality criterium the minimization of the spatial deviation from the nominal trajectory. The deterministic algorithm developed by Valenzuela and Rivas [17] is the base of the presented approach.

II. Ensemble weather forecasting

While deterministic meteorological forecasts have long been used in trajectory prediction and, as of today, are still the standard in ATM applications, a lot of efforts have been made to introduce uncertainty information in trajectory prediction systems . One of today's most promising trends in probabilistic forecasting is the use of Ensemble Prediction Systems (EPS).

An ensemble forecast comprises multiple runs of a Numerical Weather Prediction (NWP) model, which differ in the initial conditions and/or the physical parametrization of the atmosphere; some ensembles use more than one NWP model [18]. The objective is to generate a sample of possible future states of the weather outcome. An ensemble forecast is a collection of 10 to 50 forecasts (referred to as members). Cheung et al. [19] review some of them: PEARP, from Météo France, consisting of 35 members; MOGREPS, from the UK Met Office, with 12 members; the European ECMWF, with 51 members; and the multi-model ensemble SUPER, constructed by combining the previous three, forming a 98-member ensemble with the aim of capturing outliers and having a higher degree of confidence in predicting the future atmospheric evolution.

There are two approaches for trajectory prediction subject to uncertainty provided by ensemble weather forecasts:

1) Ensemble trajectory prediction, where a deterministic trajectory predictor is used for each member of the ensemble, leading to an ensemble of trajectories from which probability distributions can be derived; some type of postprocessing is required.
2) Probabilistic trajectory prediction, where probability distributions of meteorological parameters of interest (such as wind) are obtained from the ensemble forecast and evolved using a probabilistic trajectory predictor, leading to probability distributions of trajectory parameters of interest.

Cheung et al. [20] follow the first approach, and Rivas et al. [14] and this paper follow the second one.

The meteorological parameters considered in this work are the meridional (South-North), w_x, and the zonal (West-East), w_y, components of the wind. The approach to obtain the probability distributions of the wind components is as follows. Suppose that the ensemble has N members, then the first step is to obtain for each wind component and for a given location the N sample values $\{w_{x,1},...,w_{x,N}\}$ and $\{w_{y,1},...,w_{y,N}\}$. Next, one must assume that each wind component follows a particular distribution. Finally, the parameters of the chosen distribution are to be estimated from the sample.

Although the formulation presented in this paper is applicable to any probability distribution, the results shown in Section V are obtained for uniform distributions.

III. CD&R Problem formulation

A. Assumptions

The study presented in this paper is analyzed under the following assumptions (see Fig. 1):

- A North-East reference system fixed to Earth is used.
- Two aircraft, A and B, fly in the same airspace and flight level with approaching trajectories composed of several cruise segments with different courses. Instantaneous turns are assumed for course changes of the aircraft.
- The initial position of the aircraft ($\vec{s}_{0,A}$ and $\vec{s}_{0,B}$) are certain.
- The airspeeds (V_A and V_B) of both aircraft are constant and known.
- The two aircraft are affected by the same constant wind ($\vec{w}$). It is described by its meridional and zonal components (w_x and w_y, respectively) which are uncertain.
- The initial separation between the aircraft is greater than a given horizontal separation requirement D.

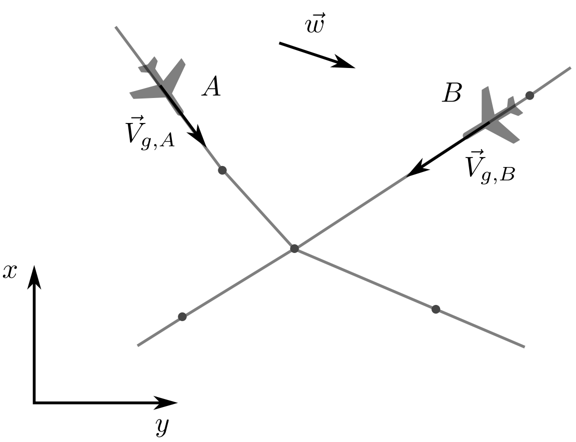

Figure 1: General scenario.

The absolute and relative motion of the aircraft are described next.

B. Aircraft motion

1) Absolute motion: Let us assume that the aircraft A and B follow trajectories composed on n and m segments, respectively. For each segment of the trajectory (see Fig. 2), the airspeeds and courses are constant and known, so the positions of the aircraft A and B in the segments $i = 1, \ldots, n$ and $j = 1, \ldots, m$ at time t, $\vec{s}_{A_i}$ and $\vec{s}_{B_j}$, are given by

$$\vec{s}_{A_i}(t) = \vec{P}_{A,o_i} + \vec{V}_{g,A_i}(t - t_{A,o_i}), \quad t \in [t_{A,o_i}, t_{Ad_i}], \tag{1}$$
$$\vec{s}_{B_j}(t) = \vec{P}_{B,o_j} + \vec{V}_{g,B_j}(t - t_{B,o_j}), \quad t \in [t_{B,o_j}, t_{B,d_j}], \tag{2}$$

where $\vec{P}_{A,o_i}$ ($\vec{P}_{B,o_j}$) is the origin waypoint of the i (j) segment; $\vec{V}_{g,A_i}$ ($\vec{V}_{g,B_j}$) is the aircraft ground speed in this segment; and t_{A,o_i} (t_{B,o_j}) and t_{A,d_i} (t_{B,d_j}) are the times on which the aircraft A (B) starts and ends the segment i (j), respectively. The time that it takes for an aircraft to fly a segment can be expressed as the length of the segment divided by the ground speed of the aircraft, as follows:

$$t_{A_i} = \frac{\|\vec{P}_{A,d_i} - \vec{P}_{A,o_i}\|}{\|\vec{V}_{g,A_i}\|}, \tag{3}$$
$$t_{B_j} = \frac{\|\vec{P}_{B,d_j} - \vec{P}_{B,o_j}\|}{\|\vec{V}_{g,B_j}\|}. \tag{4}$$

Taking this into consideration, the times when the aircraft reach the origin and destination waypoints of the segments (t_{A,o_i}, t_{A,d_i}, t_{B,o_j} and t_{B,d_j}) can be expressed as:

$$t_{A,o_i} = \sum_{p=1}^{i-1} t_{A_p}, \qquad t_{A,d_i} = \sum_{p=1}^{i} t_{A_p}, \tag{5}$$
$$t_{B,o_j} = \sum_{q=1}^{j-1} t_{B_q}, \qquad t_{B,d_j} = \sum_{q=1}^{j} t_{B_q}. \tag{6}$$

If the initial position of the aircraft ($\vec{s}_{0,A}$ and $\vec{s}_{0,B}$) are the origin waypoints of the first segments of each trajectory, then $t_{A,o_1} = t_{B,o_1} = 0$.

Because the wind is uncertain, the aircraft headings and the magnitudes of the ground speeds in each segment $\vec{V}_{g,A_i}$ and

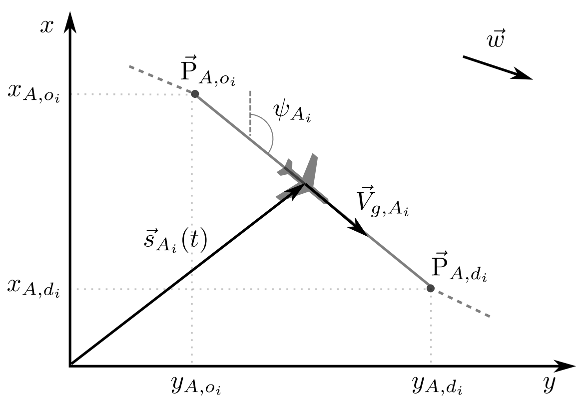

Figure 2: Absolute motion of aircraft A in segment i.

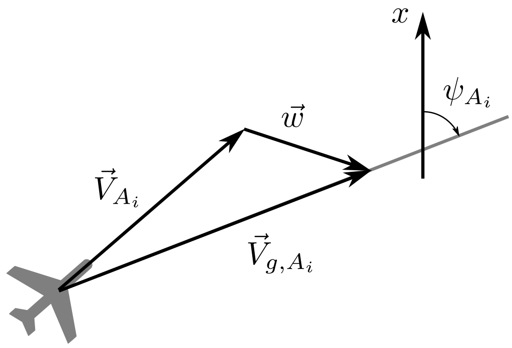

Figure 3: Wind triangle for aircraft A in segment i.

$\vec{V}_{g,B_j}$ are also uncertain. They can be obtained from the wind triangle (see Fig. 3) as follows:

$$\vec{V}_{g,A_i} = \begin{bmatrix} V_A \cos\left(\psi_{A_i} - \arcsin\left(\frac{w_{c,A_i}}{V_A}\right)\right) + w_x \\ V_A \sin\left(\psi_{A_i} - \arcsin\left(\frac{w_{c,A_i}}{V_A}\right)\right) + w_y \end{bmatrix}, \tag{7}$$
$$\vec{V}_{g,B_j} = \begin{bmatrix} V_B \cos\left(\psi_{B_j} - \arcsin\left(\frac{w_{c,B_j}}{V_B}\right)\right) + w_x \\ V_B \sin\left(\psi_{B_j} - \arcsin\left(\frac{w_{c,B_j}}{V_B}\right)\right) + w_y \end{bmatrix}, \tag{8}$$

where ψ_{A_i} and ψ_{B_j} are the aircraft courses, and w_{c,A_i} and w_{c,B_j} are the crosswinds affecting each aircraft in segments i and j, respectively. In these expressions, the crosswinds are considered to be positive if they are from the left wing, and they are given by the following expressions:

$$w_{c,A_i} = w_y \cos\psi_{A_i} - w_x \sin\psi_{A_i}, \tag{9}$$
$$w_{c,B_j} = w_y \cos\psi_{B_j} - w_x \sin\psi_{B_j}. \tag{10}$$

The aircraft courses ψ_{A_i} and ψ_{B_j} for each segment can be obtained from:

$$\psi_{A_i} = \arctan\left(\frac{y_{A,d_i} - y_{A,o_i}}{x_{A,d_i} - x_{A,o_i}}\right), \tag{11}$$
$$\psi_{B_j} = \arctan\left(\frac{y_{B,d_j} - y_{B,o_j}}{x_{B,d_j} - x_{B,o_j}}\right), \tag{12}$$

where x and y are the coordinates of the origin and destination waypoints of segments i and j, as depicted in Fig. 2.

2) Relative motion: The indicators defined in this work to characterize the conflict are only dependent of the relative motion between the aircraft, as it will be seen later. The relative position between the aircraft for segments i and j can be expressed as (from Eqs. (1) and (2)):

$$\begin{aligned}\vec{s}_{ij}(t) =& \vec{s}_{B_j}(t) - \vec{s}_{A_i}(t) = \vec{s}_{0_{ij}} + \vec{V}_{g_{ij}} t, \\ & t \in [t_{A,o_i}, t_{A,d_i}] \cap [t_{B,o_j}, t_{B,d_j}],\end{aligned} \tag{13}$$

under the condition $[t_{A,o_i}, t_{A,d_i}] \cap [t_{B,o_j}, t_{B,d_j}] \neq \emptyset$, that is, the aircraft fly the segments i and j at the same time. In the previous equation, the relative initial position, $\vec{s}_{0_{ij}}$, and the relative ground speed, $\vec{V}_{g_{ij}}$, for each pair of segments are given by

$$\vec{s}_{0_{ij}} = \vec{P}_{B,o_j} - \vec{P}_{A,o_i} - \vec{V}_{g,B_j} t_{B,o_j} + \vec{V}_{g,A_i} t_{A,o_i}, \tag{14}$$
$$\vec{V}_{g_{ij}} = \vec{V}_{g,B_j} - \vec{V}_{g,A_i}. \tag{15}$$

From equations (7) and (8), the relative ground speed can be expressed as:

$$\vec{V}_{g_{ij}} = V_B \begin{bmatrix} \cos\left(\psi_{B_j} - \arcsin\left(\frac{w_{c,B_j}}{V_B}\right)\right) \\ \sin\left(\psi_{B_j} - \arcsin\left(\frac{w_{c,B_j}}{V_B}\right)\right) \end{bmatrix} - V_A \begin{bmatrix} \cos\left(\psi_{A_i} - \arcsin\left(\frac{w_{c,A_i}}{V_A}\right)\right) \\ \sin\left(\psi_{A_i} - \arcsin\left(\frac{w_{c,A_i}}{V_A}\right)\right) \end{bmatrix}. \quad (16)$$

Notice that both $\vec{V}_{g_{ij}}$ and $\vec{s}_{0_{ij}}$ are uncertain due to the wind uncertainty.

C. Conflict detection

A conflict exists between two aircraft if a given set of separation minima is predicted to be violated in the future. In this project it is assumed that both aircraft are flying at the same flight level and that they are approaching, so a conflict will exist if the minimum distance between them, d_{min}, is found to be smaller than a given horizontal separation requirement. In this paper, the conflict between the aircraft is characterized by two indicators: the minimum distance between the aircraft, d_{min}, and the probability of conflict, P_{con}. The probabilistic conflict detection problem is tackled using the Probabilistic Transformation Method (PTM), later described in Section IV. Using this method, it is possible to obtain the probability density function (PDF) of the conflict indicator $f_{d_{min}}$, as well as the value of P_{con}.

The distance between the aircraft A flying in segment i and the aircraft B flying in segment j, $d_{ij}(t)$, is the magnitude of the relative position, $d_{ij}(t) = \|\vec{s}_{ij}(t)\|$. It can be expressed as

$$d_{ij}(t) = \sqrt{s_{0_{ij}}^2 + 2\vec{s}_{0_{ij}} \cdot \vec{V}_{g_{ij}} t + V_{g_{ij}}^2 t^2}, \quad t \in [t_{A,o_i}, t_{A,d_i}] \cap [t_{B,o_j}, t_{B,d_j}]. \quad (17)$$

A loss of separation would take place if $d_{ij}(t)$ were to be smaller than the separation requirement D. Because $\vec{s}_{0_{ij}}$ and $\vec{V}_{g_{ij}}$ are uncertain, so they are $d_{ij}(t)$ and, therefore, the existence of a loss of separation at a given time. The indicators that characterize the conflict are described next:

1) Minimum distance: For each pair of segments $i = 1, \ldots, n$ and $j = 1, \ldots, m$, the minimum distance between the aircraft $d_{min,ij}$ can be obtained from Eq. (17) as

$$d_{min,ij} = \sqrt{s_{0_{ij}}^2 + 2\vec{s}_{0_{ij}} \cdot \vec{V}_{g_{ij}} t_{d_{min},ij} + V_{g_{ij}}^2 t_{d_{min},ij}^2}. \quad (18)$$

In this equation, $t_{d_{min},ij}$ is the time to minimum distance (or time of maximum approach) for each pair of segments, that can be expressed as:

$$t_{d_{min},ij} = \begin{cases} \max\{t_{A,o_i}, t_{B,o_j}\} & \text{if } t_{ij}^* < \max\{t_{A,o_i}, t_{B,o_j}\} \\ t_{ij}^* & \text{if } t_{ij}^* \in [t_{A,o_i}, t_{A,d_i}] \cap [t_{B,o_j}, t_{B,d_j}] \\ \min\{t_{A,d_i}, t_{B,d_j}\} & \text{if } t_{ij}^* > \min\{t_{A,d_i}, t_{B,d_j}\} \end{cases}, \quad (19)$$

where t_{ij}^* is the time obtained by setting to zero the derivative of Eq. (17) with respect to t:

$$t_{ij}^* = \frac{-\vec{s}_{0_{ij}} \cdot \vec{V}_{g_{ij}}}{V_{g_{ij}}^2}. \quad (20)$$

Finally, the value of the indicator d_{min} is the minimum value of the set $\{d_{min,ij}\}$:

$$d_{min} = \min\{d_{min,ij}\}. \quad (21)$$

2) Probability of conflict: The probability of existence of a conflict is given by the probability of d_{min} being smaller than the separation requirement D:

$$P_{con} = P[d_{min} \leq D] \quad (22)$$

Notice that these two indicators depend on the wind, and therefore are affected by its uncertainty.

D. Conflict resolution

The conflict resolution process is designed in such a way that it generates a trajectory for each aircraft that present a probability of conflict smaller than a given threshold P_0. These resolution trajectories are defined by a new set of waypoints (vectoring). Considering that the nominal paths of the aircraft are the preferred trajectories, the deconflicted trajectories are determined so that they are as close as possible to the originals. The CR process herein presented is based on the deterministic algorithm developed by Valenzuela and Rivas in [17].

The conflict resolution problem is then formulated as a parametric optimization problem subject to inequality constraints:

$$\begin{aligned} &\text{minimize the cost function} && F(\mathbf{x}) \\ &\text{subject to the contraints} && c(\mathbf{x}) \leq \mathbf{0}. \end{aligned} \quad (23)$$

1) Parameters: The resolution trajectory is described in terms of a set of parameters $\mathbf{x}$, which correspond to the coordinates of the modifiable waypoints. Considering that the first and last waypoints of each trajectory remain fixed, the total number of modifiable waypoints is $q = n + m - 4$.

$$\mathbf{x} = [x_{A,2}, \ldots, x_{A,n-1}, y_{A,2}, \ldots, y_{A,n-1}, x_{B,2}, \ldots, x_{B,m-1}, y_{B,2}, \ldots, y_{B,m-1}]^{\mathrm{T}}. \quad (24)$$

2) Cost Function: The optimality criterium in this problem is to minimize the deviation of the resolution trajectories from the nominal trajectories, which is defined as the following objective function:

$$F(x) = \sqrt{\sum_{k=1}^{q} \left[(x_k - x_k^n)^2 + (y_k - y_k^n)^2\right]}, \quad (25)$$

where (x_k^n, y_k^n) are the nominal coordinates of the modifiable waypoints.

3) Constraints: In the problem under consideration, the sole constrain is the condition for the probability of conflict P_{con} of being smaller than P_0. This inequality constraint can be expressed as:

$$c(\mathbf{x}) = P_{con}(\mathbf{x}) - P_0 \leq 0. \quad (26)$$

4) Resolution Strategy: The resolution process has two phases:

1. Search of a Feasible Starting Point: In this phase, the objective is to find a starting point $\mathbf{x_0}$ that satisfies the inequality constraint. This starting point is obtained by solving the following unconstrained optimization problem:

$$\text{minimize } P_{con}(\mathbf{x}). \tag{27}$$

Taking into account that the minimum of the function $P_{con}(\mathbf{x})$ is zero, the constrain (26) is guaranteed to be satisfied by this solution. The nominal trajectory $\mathbf{x}^n$ is chosen as the starting point in this problem.

2. Cost Function Optimization: Once an initial feasible point is obtained, the aim of this second phase is to obtain the feasible solution with the smaller cost by solving the parametric optimization problem described in Eq. (23).

Considering that both the cost function and the constraint are non-linear, the optimization problem can be described as a nonlinear programming problem. Each phase of the resolution problem is carried out using MATLAB's nonlinear programming solvers *fminunc* and *fmincon*, for phase one and two, respectively.

IV. Probabilistic Transformation Method

The probability density function (PDF) of the conflict indicator d_{min}, given a wind speed probability distribution, is obtained using the Probabilistic Transformation Method (PTM). An introduction to the application of this method to the problem of conflict detection under wind uncertainty was presented in Hernández et al. [16].

The basis of this transformation is as follows (see, for example, Ref. [15]): Let u_1 and u_2 be two continuous-type random variables, statistically correlated or independent, having a joint PDF $f_{u_1,u_2}(u_1,u_2)$, and let R be the two-dimensional region in the u_1u_2-plane where $f_{u_1,u_2}(u_1,u_2) > 0$. Let v_1 and v_2 be two random variables, $v_1 = g_1(u_1,u_2)$ and $v_2 = g_2(u_1,u_2)$, whose PDFs are to be found. Assuming that $g_1(u_1,u_2)$ and $g_2(u_1,u_2)$ define a one-to-one transformation of R onto a region S in the v_1v_2-plane, then u_1 and u_2 can be expressed in terms of v_1 and v_2 as $u_1 = h_1(v_1,v_2)$ and $u_2 = h_2(v_1,v_2)$. The joint PDF of v_1 and v_2 is then given by

$$f_{v_1,v_2}(v_1,v_2) = \begin{cases} f_{u_1,u_2}(h_1(v_1,v_2),h_2(v_1,v_2))\,|J(v_1,v_2)| & \text{if } (v_1,v_2) \in S \\ 0 & \text{otherwise.} \end{cases} \tag{28}$$

In this expression, $|J(v_1,v_2)|$ is the absolute value of the Jacobian determinant

$$J(v_1,v_2) = \begin{vmatrix} \dfrac{\partial h_1(v_1,v_2)}{\partial v_1} & \dfrac{\partial h_1(v_1,v_2)}{\partial v_2} \\ \dfrac{\partial h_2(v_1,v_2)}{\partial v_1} & \dfrac{\partial h_2(v_1,v_2)}{\partial v_2} \end{vmatrix}, \tag{29}$$

which is assumed to be different from zero in S.

In this work, the variables u_1 and u_2 are the two wind components w_x and w_y, respectively; v_1 is the indicator d_{min}; and v_2 is an auxiliary variable which, in order to simplify the Jacobian determinant, is chosen to be any of the two initial random variables u_1 or u_2 (i.e., the wind components w_x or w_y), resulting in $J = -\partial h_2(v_1,v_2)/\partial v_1$ or $J = \partial h_1(v_1,v_2)/\partial v_1$, respectively.

The marginal PDF of d_{min}, $f_{d_{min}}(d_{min})$, can be obtained from the joint PDF $f_{d_{min},v_2}(d_{min},v_2)$ as follows

$$f_{d_{min}}(d_{min}) = \int_{-\infty}^{\infty} f_{d_{min},v_2}(d_{min},v_2)\mathrm{d}v_2. \tag{30}$$

Once the PDF $f_{d_{min}}(d_{min})$ is known, one can compute the mean and the standard deviation of d_{min}:

$$E[d_{min}] = \int_{-\infty}^{\infty} \rho f_{d_{min}}(\rho)\mathrm{d}\rho, \tag{31}$$

$$\sigma[d_{min}] = \left[\int_{-\infty}^{\infty} \rho^2 f_{d_{min}}(\rho)\mathrm{d}\rho - \left(E[d_{min}]\right)^2\right]^{1/2}. \tag{32}$$

This procedure is only to be applied when the transformations g_1 and g_2 are invertible functions in the domain of f_{u_1,u_2}. However, it may happen that different wind values lead to the same value of the indicator and the auxiliary variable, thus having a more-to-one transformation. When this situation arises, the problem is divided into multiple sets S_j where the transformation is one-to-one, and the procedure is applied to each domain.

The probability of conflict can be computed from the PDF of d_{min} obtained with the PTM as

$$P_{con} = \int_{-\infty}^{D} f_{d_{min}}(\rho)\mathrm{d}\rho. \tag{33}$$

V. Results

Some initial results are presented for a particular scenario and arbitrary winds distributed uniformly.

The scenario under consideration presents two aircraft with segmented trajectories approaching to a common navigation point. The nominal trajectories of aircraft A and B are depicted in Fig. 4, and correspond to RNAVs routes UM192 and UN869, respectively. The waypoints latitudes and longitudes are collected in Table I; these coordinates can be consulted in [21] and [22]. The waypoints coordinates have been transformed to a North-East reference system fixed to Earth whose origin is the waypoint BLN, using an azimuthal equidistant projection. The initial position of aircraft A is $\vec{s}_{0,A} = [-78.74, 65.63]$ NM, which corresponds to waypoint AMR; and the initial position of aircraft B is $\vec{s}_{0,B} = [74.94, 27.71]$ NM, waypoint NASOS. The horizontal separation requirement D is set to 5 NM (9260 m) and the airspeeds of the aircraft A and B to $V_A = 240$ m/s and $V_B = 230$ m/s. The probability of conflict threshold set in the CR process is $P_0 = 0.1\%$

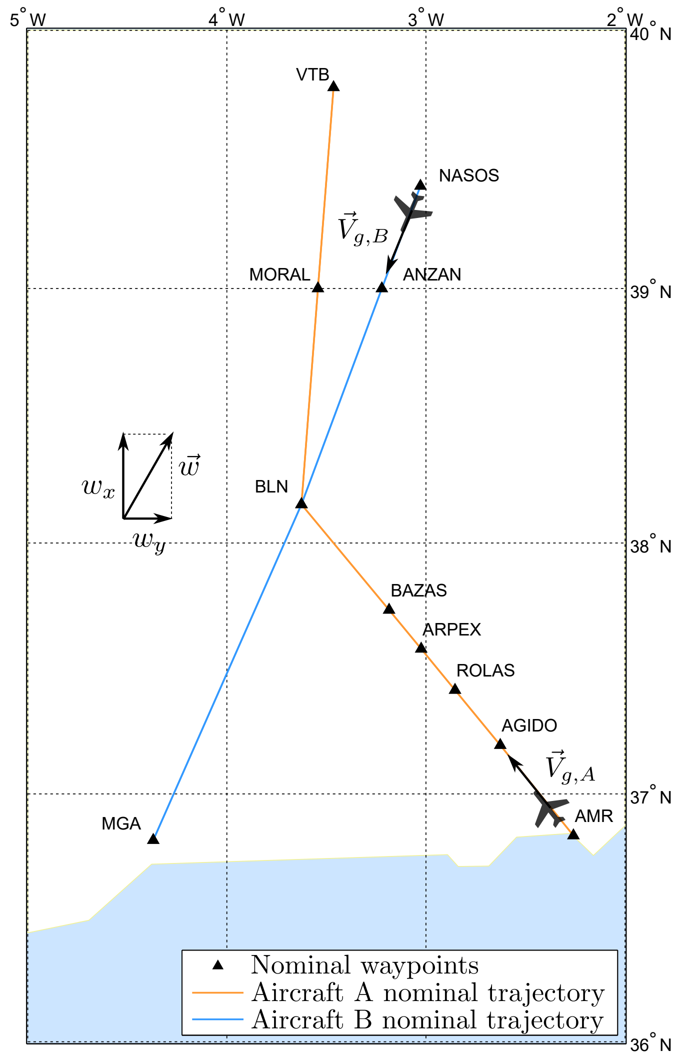

Figure 4: Nominal scenario.

The wind components are considered to be statistically independent and distributed as uniform continuous random variables, whose PDFs are given by:

$$f_{w_i}(w_i) = \begin{cases} \frac{1}{2\delta_{w_i}}, & \text{if } w_i \in [\bar{w}_i - \delta_{w_i}, \bar{w}_i + \delta_{w_i}] \\ 0 & \text{otherwise,} \end{cases} \quad (34)$$

where $i \in \{x, y\}$. Since the winds are independent, the joint PDF of the wind components is the product of these two PDFs,

$$f_{w_x,w_y}(w_x, w_y) = f_{w_x}(w_x) f_{w_y}(w_y). \quad (35)$$

The endpoints of the uniform distributions are chosen to be the maximum and minimum values of the forecasted winds provided by the EPS. In this application, the meteorological uncertainty data is retrieved from the European Centre for Medium-Range Weather Forecasts. In particular, the PEARP weather forecast, composed of 35 members, is considered. The wind available is the one given for a forecast horizon of 0 hours, released at 06:00 on 05-May-2016, for a pressure

TABLE I: WAYPOINTS DESIGNATORS AND NOMINAL COORDINATES.

Aircraft A trajectory		**Aircraft B trajectory**	
Designator	Coordinates	Designator	Coordinates
AMR	36 49 59.4 N 002 15 33.9 W	NASOS	39 23 56.9 N 003 01 40.0 W
AGIDO	37 11 44.5 N 002 37 37.0 W	ANZAN	39 00 00.0 N 003 13 17.2 W
ROLAS	37 24 56.3 N 002 51 15.7 W	BLN	38 09 09.1 N 003 37 30.0 W
ARPEX	37 34 47.1 N 003 01 27.1 W	MGA	36 48 51.5 N 004 22 10.5 W
BAZAS	37 44 03.9 N 003 11 06.7 W		
BLN	38 09 09.1 N 003 37 30.0 W		
MORAL	39 00 00.0 N 003 32 31.8 W		
VTB	39 46 50.6 N 003 27 51.1 W		

level of 250 hPa, and for the coordinates 38° North, 2.5° West, in the Southeast of Spain. The minimum and maximum values of w_x are 11.75 and 28.40 m/s, respectively, and the minimum and maximum values of w_y are 10.24 and 25.54 m/s, respectively. The corresponding values of the wind distributions are $\bar{w}_x = 20.08$ m/s, $\delta_{w_x} = 8.33$ m/s, $\bar{w}_y = 17.89$ m/s, and $\delta_{w_y} = 7.65$ m/s. Figure 5 depicts the winds probability density functions, along with the normalized bar charts that represent the PEARP weather forecast data.

In Figure 6, the PDFs of the minimum distance d_{min} before and after the conflict resolution process are presented. The PDF corresponding to the nominal scenario is depicted with a dashed line, and a solid line is used to represent the PDF for the resolution trajectories.

The expected value and standard deviation of d_{min} for the nominal trajectories are $E[d_{min}] = 7044$ m and $\sigma[d_{min}] = 3170$ m. The probability of conflict before the CR is 70.4%, which can be computed as the area under the PDF to the left of the dash-dot vertical line that represent the separation requirement D. After the conflict resolution process, the expected value and standard deviation have changed to 14329 m and 2897 m, respectively. It is noticeable that the expected value has experienced a significant raise and that the dispersion of the indicator is now slightly smaller. The probability of conflict has dropped to $P_{con} = 0.1\%$, which correspond to the constraint set in the CR process. As observed in the figure, the nominal and resolution PDFs are very similar in shape, being the main difference between the two of them their position on the x axis.

The resolution trajectories for each aircraft are depicted in Figure 7, where the new trajectories have been depicted with solid lines. The cost of this solution (see Eq. 25) is $F = 6973$ m. The maximum deviation from its nominal tra-

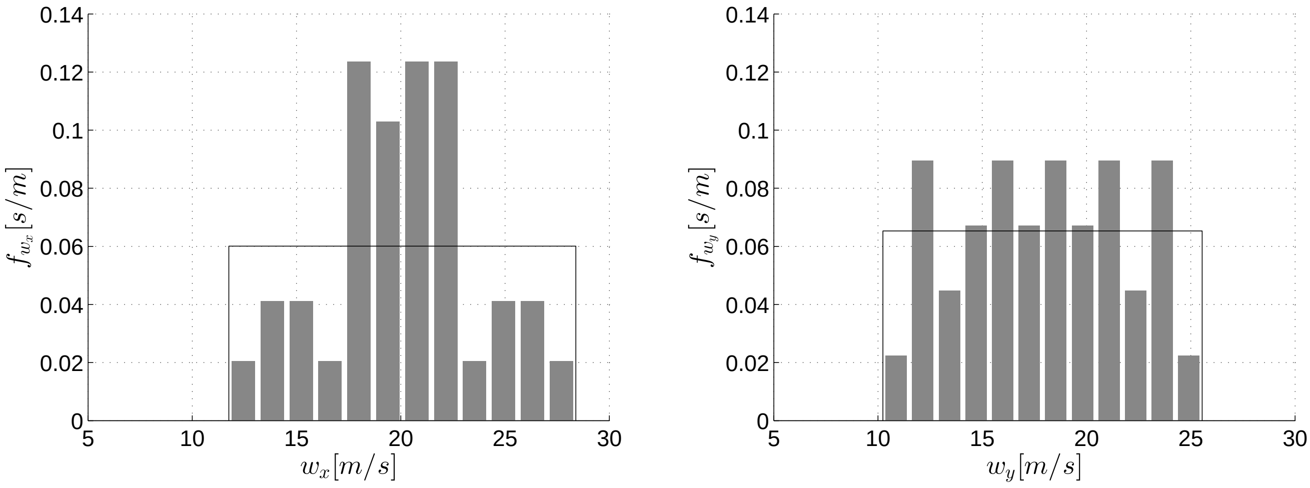

(a) Wind meridional component.

(b) Wind zonal component.

Figure 5: Wind probability distributions (solid lines) and PEARP weather forecast normalized data (bars).

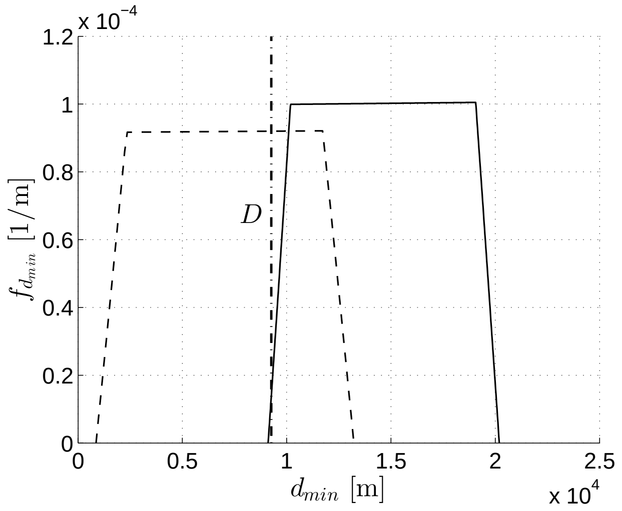

Figure 6: PDF of d_{min} for nominal (dashed) and resolution (solid) trajectories.

jectory is 4826 m for the aircraft A and 5029 m for aircraft B. This maximum deviation correspond to the waypoints closer to the navigation point BLN. It can be observed that the rest of the modifiable waypoints have not experienced noticeable changes.

VI. Conclusions

In this work, a probabilistic method for conflict detection and resolution for en route aircraft under wind uncertainty has been presented. The proposed method allows the characterization of a conflict between two aircraft and it is able to propose new trajectories that lower the probability of conflict to acceptable levels.

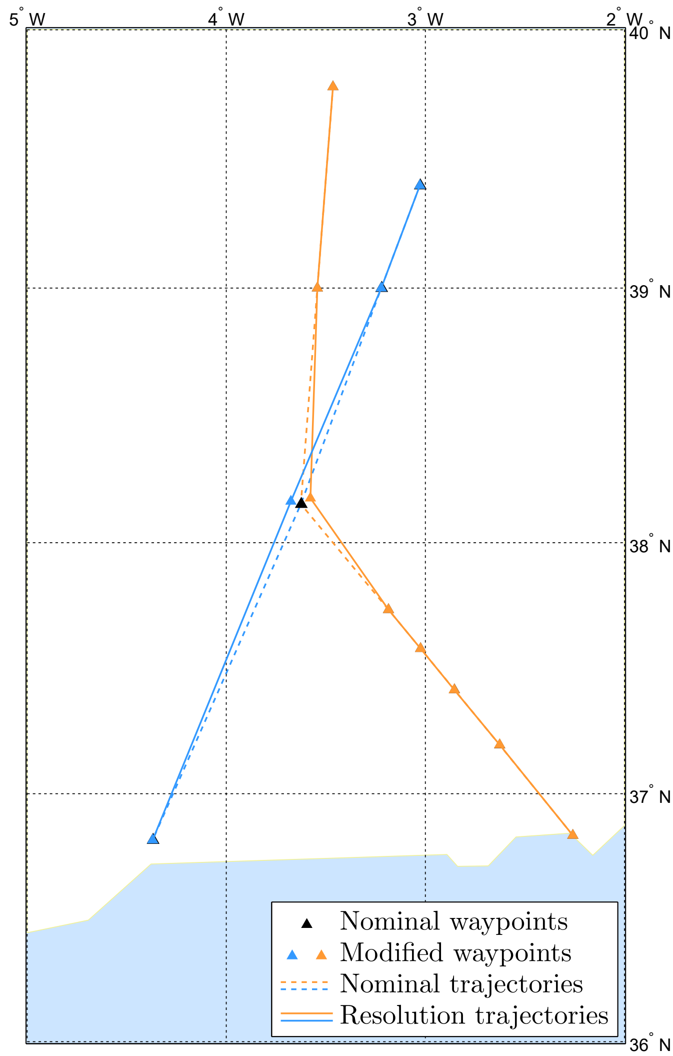

Figure 7: Resolution trajectories.

The probabilistic conflict detection problem has been tackled using the Probabilistic Transformation Method. This methodology enables the assessment of the probability of conflict and other characteristics of the conflict for a given scenario. This approach is capable of taking as input any type of wind distribution derived from ensemble weather forecast. The minimum distance between the aircraft and the probability of conflict have been chosen as indicators to characterize the conflict.

The conflict resolution problem has been formulated as a parametric optimization problem and it is based on the modification of the nominal waypoints of the aircraft trajectories. With the proposed CR process it is possible to obtain a new set of trajectories with an acceptable value of the conflict probability and with a minimum deviation from the nominal trajectories.

The method has been applied to a particular scenario and some numerical results has been presented. A uniform wind distribution has been considered for the numerical application. The uncertainty information to determine the wind probability density function has been obtained from weather ensemble forecasting.

The consideration of different types of wind probability distributions or correlated wind-fields in which the wind velocity varies with the position is left for future work. The employment of wind information sources different from the EPS could also be of great interest. Next steps in this line of investigation also include the task of considering trajectories with altitude and velocity changes, of potential application to Terminal Maneuvering Areas.

Acknowledgments

The authors gratefully acknowledge the financial support of the Spanish Ministerio de Economía y Competitividad through Grant TRA2014-58413-C2-1-R, co-financed with FEDER funds.

References

[1] D. Rivas and R. Vazquez, “Uncertainty,” in Complexity Science in Air Traffic Management, A. Cook and D. Rivas Ed., Ashgate Publishing Limited, 2016, Chap. 4.

[2] Q.M. Zheng and Y.J. Zhao, “Modeling Wind Uncertainties for Stochastic Trajectory Synthesis,” 11th AIAA Aviation Technology, Integration, and Operations (ATIO) Conference, paper AIAA 2011-6858, 2011, pp. 1–10. doi:10.2514/6.2011-6858

[3] A. Nilim, L. El Ghaoui, M. Hansen, and V. Duong, “Trajectory-based Air Traffic Management (TB-ATM) under Weather Uncertainty,” Proc. 4th USA/Europe Air Traffic Management Research and Development Seminar (ATM-2001), Santa Fe, NM, 2001, pp. 1–11.

[4] R.A. Paielli and H. Erzberger, “Conflict Probability Estimation for Free Flight,” *Journal of Guidance, Control, and Dynamics*, Vol. 20, No. 3, 1997, pp. 588–596. doi: 10.2514/6.1997-1

[5] J. Krozel and M. Peters, “Strategic Conflict Detection and Resolution for Free Flight,” Proc. 36th IEEE Conference on Decision and Control, San Diego, CA, 1997, pp. 1822-1828.

[6] M. Prandini, J. Hu, J. Lygeros, and S. Sastry, “A Probabilistic Approach to Aircraft Conflict Detection,” *IEEE Transactions on Intelligent Transportation Systems*, Vol. 1, No. 4, 2000, pp. 199–220. doi: 10.1109/6979.898224

[7] J. Hu, M. Prandini, and S. Sastry, “Aircraft Conflict Prediction in the Presence of a Spatially Correlated Wind Field,” *IEEE Transactions on Intelligent Transportation Systems*, Vol. 6, No. 3, 2005, pp. 326–340. doi: 10.1109/TITS.2005.853699

[8] G. Chaloulos and J. Lygeros, “Effect of wind correlation on aircraft conflict probability,” *Journal of Guidance, Control, and Dynamics*, vol. 30, no. 6, 2007, pp. 1742–1752.

[9] Y. Matsuno, T. Tsuchiya, J. Wei, I. Hwang, and N. Matayoshi, “Stochastic optimal control for aircraft conflict resolution under wind uncertainty,” *Aerospace Science and Technology*, vol. 43, 2015, pp. 77 – 88.

[10] Y. Matsuno, T. Tsuchiya, and N. Matayoshi, “Near-optimal control for aircraft conflict resolution in the presence of uncertainty,” *Journal of Guidance, Control, and Dynamics*, vol. 39, 2016, pp. 326–338.

[11] O. Rodionova, B. Sridhar, and H. K. Ng, “Conflict resolution for wind-optimal aircraft trajectories in north atlantic oceanic airspace with wind uncertainties,” in *Digital Avionics Systems Conference (DASC), 2016 IEEE/AIAA 35th*, IEEE, 2016, pp. 1–10.

[12] D. González-Arribas, M. Soler, M. Sanjurjo, “Wind-based robust trajectory optimization using meteorological ensemble probabilistic forecasts”, Proc. 6th SESAR Innovation Days (SID2016), 2016, pp. 1-8.

[13] M. Steiner, R. Bateman, D. Megenhardt, Y. Liu, M. Pocernich, and J.A. Krozel, “Translation of Ensemble Weather Forecasts into Probabilistic Air Traffic Capacity Impact,” *Air Traffic Control Quarterly*, Vol. 18, 2010, pp. 229–254.

[14] D. Rivas, A. Franco, and A. Valenzuela, “Analysis of aircraft trajectory uncertainty using Ensemble Weather Forecasts”, Proc. 7th European Conference for Aeronautics and Space Sciences (EUCASS), 2017, pp. 1-12.

[15] R.V. Hogg and A.T. Craig, “Introduction to Mathematical Statistics,” Prentice-Hall International, Englewood Cliffs, N.J., 1995, pp. 168–178.

[16] E. Hernández, A. Valenzuela, and D. Rivas, “Probabilistic Aircraft Conflict Detection Considering Ensemble Weather Forecast,” Proc. 6th SESAR Innovation Days (SID2016), Delft, Netherlands, 2016, pp. 1–8.

[17] A. Valenzuela and D. Rivas, “Conflict Resolution in Converging Air Traffic Using Trajectory Patterns,” *Journal of Guidance, Control, and Dynamics*, vol. 34, July 2011, pp. 1172–1189.

[18] World Meteorological Organization, “Guidelines on Ensemble Prediction Systems and Forecasting,” WMO-No. 1091, 2012.

[19] J. Cheung, A. Hally, J. Heijstek, A. Marsman, and J.-L. Brenguier, “Recommendations on Trajectory Selection in Flight Planning based on Weather Uncertainty,” Proc. 5th SESAR Innovation Days (SID2015), Bologna, Italy, 2015, pp. 1–8.

[20] J. Cheung, J.-L. Brenguier, J. Heijstek, A. Marsman, and H. Wells, “Sensitivity of flight durations to uncertainties in numerical weather predictions”, Proceedings of the 4th SESAR Innovation Days (SID2014), 2014, pp. 1-8.

[21] Aeronautical Information Service Spain, “Aeronautical Information Publication Spain. 4.1 En Route, Radio Navigation Aids”, May 2017.

[22] Aeronautical Information Service Spain, “Aeronautical Information Publication Spain. 4.4 En Route, Name-Code Designators for Significant Routes”, April 2017.